A multi-sensory code for emotional arousal: supplementary information

Beau Sievers[a], Caitlyn Lee[b], William Haslett[c] & Thalia Wheatley[b]

[a]Department of Psychology, Harvard University, Cambridge, MA 02138
[b]Department of Psychological and Brain Sciences, Dartmouth College, Hanover, NH 03755
[c]Department of Biomedical Data Science, Geisel School of Medicine at Dartmouth, Hanover, NH 03755

Correspondence to: Thalia Wheatley, 6207 Moore Hall, Dartmouth College, Hanover, NH 03755. thalia.p.wheatley@dartmouth.edu

Data, code, and materials

Data, code, and materials for all studies and analyses can be downloaded at: https://github.com/beausievers/supramodal_arousal

Power analysis

We performed a power analysis based on Davis's (1961) test of the *Bouba–Kiki* paradigm (using the words *takete* and *uloomu*) in a population of school children in Tanganyika (N=131). A reanalysis of Davis's data using Fisher's exact test of proportion yielded an observed effect size of g=.23, indicating 58 participants were required for 95% power. Accordingly, the minimum sample size for each between-subjects task was set to N=60. For within-subjects tasks, we lacked a pre-existing basis for power analysis, and so chose to use a much larger number of trials to ensure we could detect small-to-medium sized effects for each participant (Study 3: 520 trials per participant, 19,630 total trials; Study 5: 220 trials per participant, 10,934 total trials).

Bayesian modeling

The Bayesian model used in Study 1 estimated the likelihood of a congruent outcome using a binomial distribution with parameters n, k, and θ, where n is the total number of trials, k is the number of congruent trials, and θ is the success rate, or the probability of a congruent result. We selected a flat beta prior probability distribution, reflecting the possibility that though the behavior of the participant population could match expectations, they could just as likely perform at chance or possess consistent sound–shape associations opposite previous research. We estimated the posterior distribution of θ given our data using Monte Carlo Markov Chain simulation with JAGS (Plummer, 2003) for R (R Core Team, 2014).

Studies 2 and 4 used a Bayesian generalized linear model with a logit link function and two parameters: the intercept α and slope β. Noninformative uniform priors were used. The posterior distributions of α and β were estimated using STAN (Carpenter et al., in press) and PyStan (http://mc-stan.org/).

Study 3 used a Bayesian generalized linear model with a logit link function and parameters corresponding to each model predictor and each possible interaction between predictors (including three- and four-way interactions). All models included random slopes and intercepts per participant for all parameters and interactions. Posterior distributions were modeled using BAMBI (Yarkoni & Westfall, 2016) and PyMC3 (Salvatier, Wiecki, & Fonnesbeck, 2016). BAMBI's default "smart" weakly informative priors were used, shrinking parameter estimates toward zero.

Study 5 used a Bayesian generalized linear model with parameters as described in the main text, and was modeled using BAMBI and "smart" priors as in Study 3.

Harris corner detection

Before detecting corners, images were converted to 8-bit grayscale and smoothed using a median filter (to remove irregularities caused by differences in pen pressure, dust on the scanner, etc.), and gamma corrected. The Harris corner detection algorithm requires four parameters: k, a sensitivity factor for separating corners from edges; ε, a normalization factor; σ, the standard deviation of a Gaussian kernel, which is used as a weighting function; and a minimum distance between corners. For the first survey, images were scanned at 600 pixels per inch along both axes. After completing the first free-drawing survey, our department replaced its copier/scanner, and so for the second survey, images were scanned at 200 pixels per inch along both axes. Because the effects of the image processing and Harris corner detection parameters are resolution- and scanner-dependent, we used different settings for the first and second surveys. Within each survey, all images were processed using the same settings regardless of emotion content. Images from the first survey were smoothed using a median filter with a five-pixel radius, gamma corrected by a factor of 5, and used $k = .05$, $\varepsilon = .000006$, $\sigma = 15$, and a 20px minimum distance between corners for Harris corner detection. Images from the second survey were smoothed using a median filter with a one-pixel radius, were not gamma corrected, and used $k = .05$, $\varepsilon = .000006$, $\sigma = 5$, and a 20px minimum distance between corners for Harris corner detection. Image processing was performed using Scikit-Image (van der Walt et al., 2014).

Additional PBML analysis

To determine whether all joints communicated arousal with equal effectiveness, we conducted linear discriminant analysis per joint, using stratified 10-fold cross validation. Ten of fifteen individual joints had higher accuracy than the wholebody analysis (M = 89%, range: 86%–93%), suggesting relationships between joint-axis features interfered with rather than increased classification accuracy. This indicates coarse differences in SC within individual joints best predicted emotional arousal.

Study 4: Procedurally generated stimuli

Shapes. Shapes were created using one of two algorithms. The first algorithm randomly placed a number of vertices, then connected those vertices with either a randomly parameterized Bezier curve or a straight line. The second algorithm randomly placed a number of vertices both on and near the circumference of a circle, then connected those points in counter-clockwise order using a single curve.

Sounds. Sounds were created using one of three algorithms. The first algorithm used a sine wave oscillator modulated by a feedback network of low-frequency oscillators with variable wave shapes. The second algorithm used a sawtooth oscillator with randomly varied harmonics. The third algorithm used a Rössler attractor (Rössler, 1976) modulated by a randomly parameterized sine wave oscillator. All stimuli were generated using Pyo (Belanger, 2016).

Study 4: Model summaries

Summary tables for all models including means, standard deviations, and 95% credible intervals for all parameters and interactions are included as an attachment.

Study 4: All model plots

Plots of the posterior probability of high arousal emotion judgment for the largest fixed main effect in each model are included below.

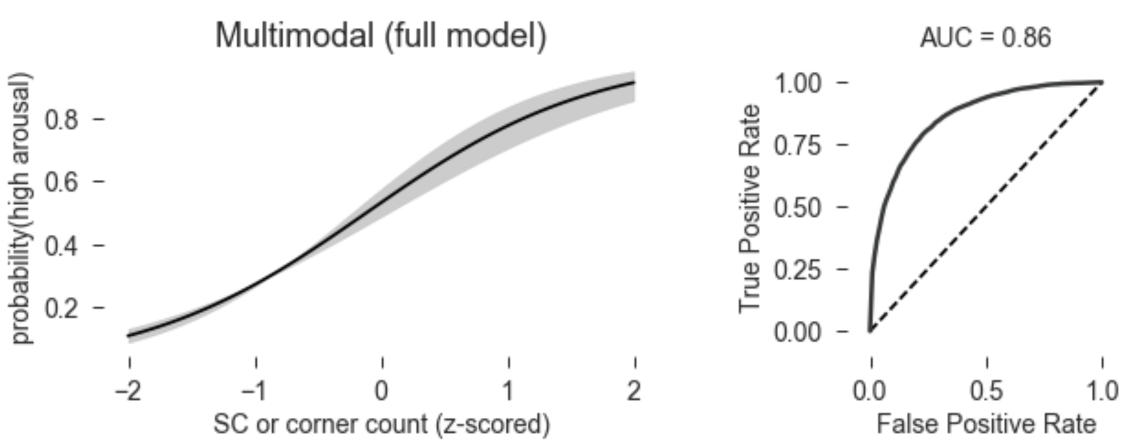

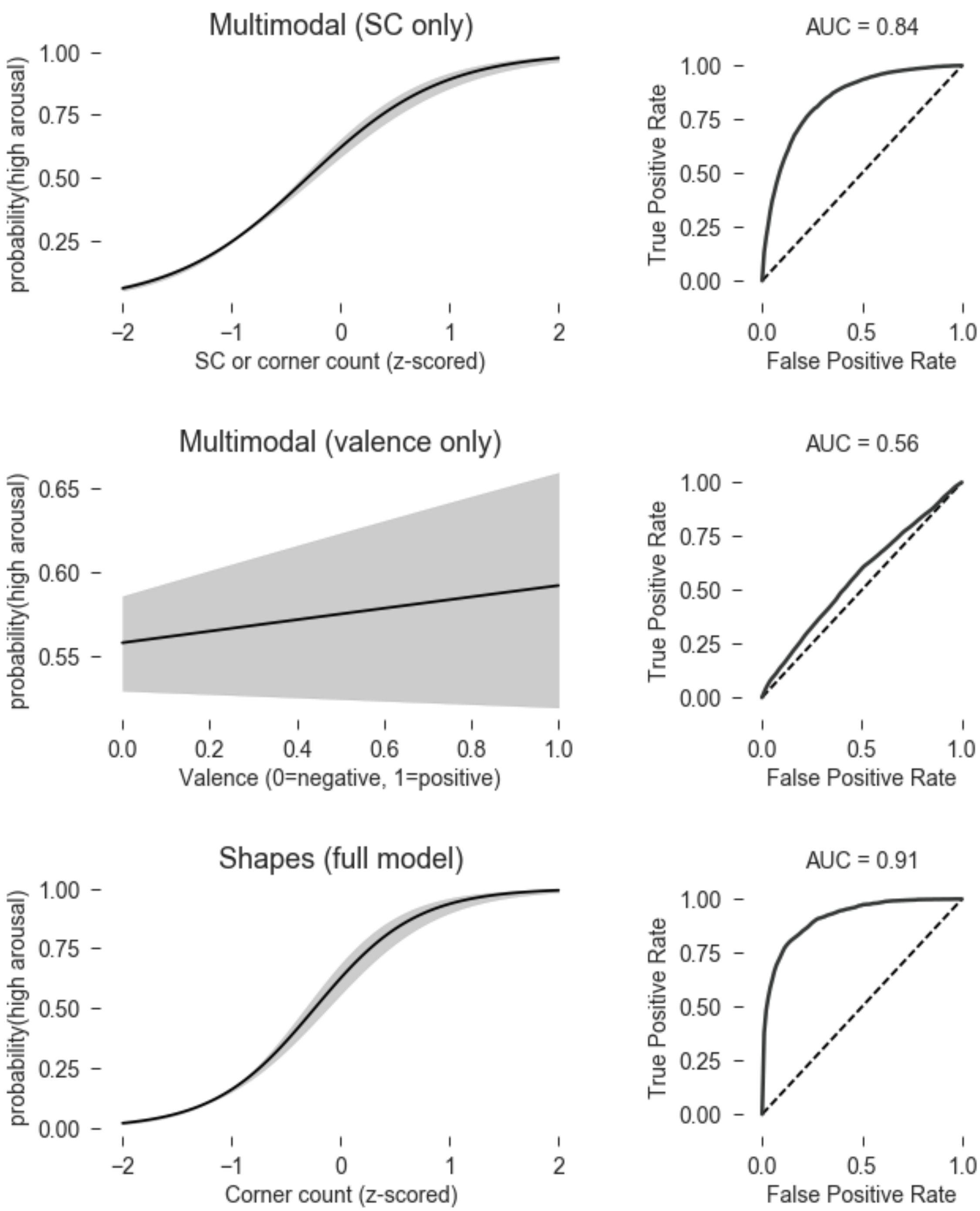
Multimodal (SC only)
probability(high arousal)
SC or corner count (z-scored)
AUC = 0.84
True Positive Rate
False Positive Rate
Multimodal (valence only)
probability(high arousal)
Valence (0=negative, 1=positive)
AUC = 0.56
True Positive Rate
False Positive Rate
Shapes (full model)
probability(high arousal)
Corner count (z-scored)
AUC = 0.91
True Positive Rate
False Positive Rate

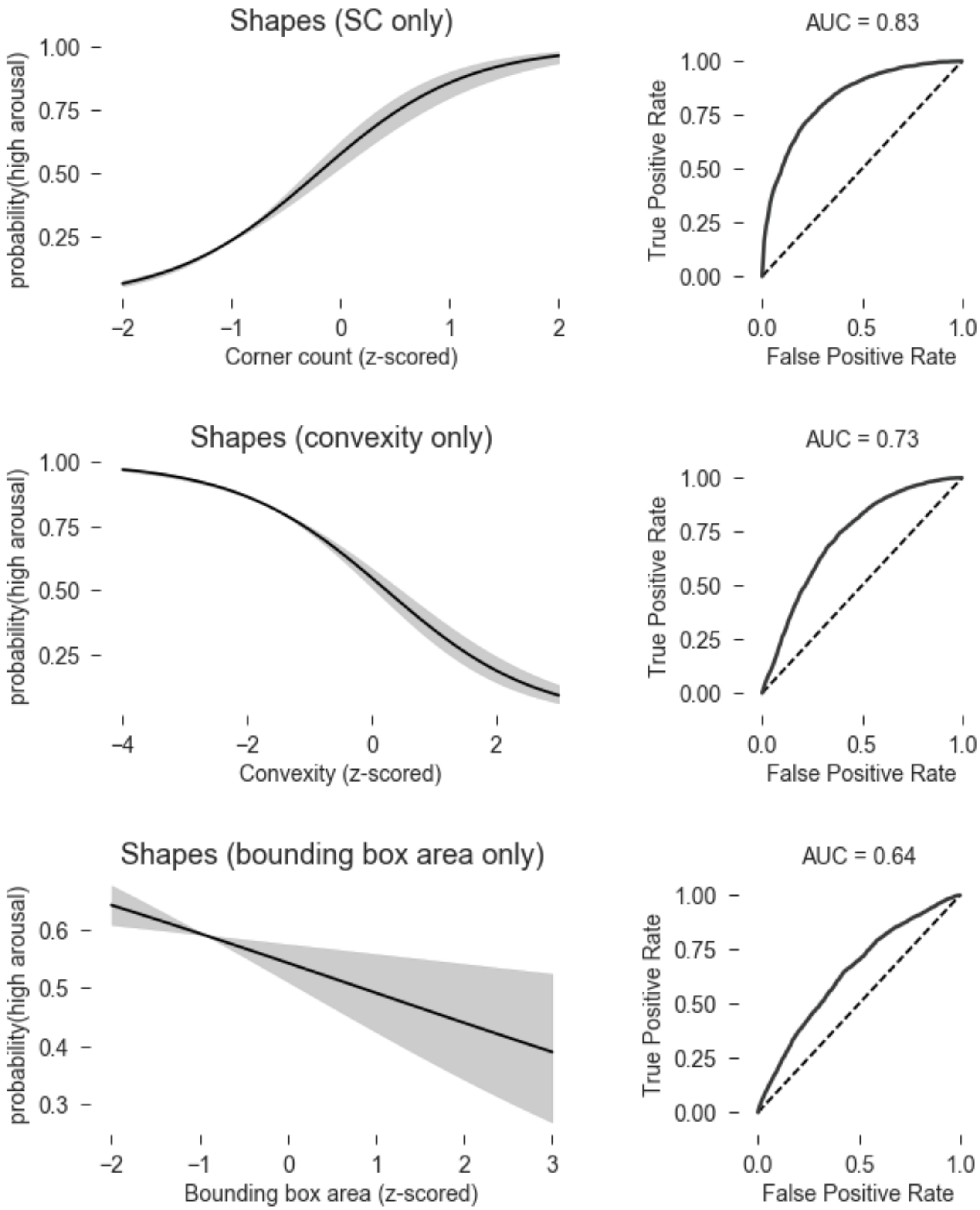
Shapes (SC only)
probability(high arousal)
1.00
0.75
0.50
0.25
−2
−1
0
1
2
Corner count (z-scored)
AUC = 0.83
True Positive Rate
1.00
0.75
0.50
0.25
0.00
0.0
0.5
1.0
False Positive Rate
Shapes (convexity only)
probability(high arousal)
1.00
0.75
0.50
0.25
−4
−2
0
2
Convexity (z-scored)
AUC = 0.73
True Positive Rate
1.00
0.75
0.50
0.25
0.00
0.0
0.5
1.0
False Positive Rate
Shapes (bounding box area only)
probability(high arousal)
0.6
0.5
0.4
0.3
−2
−1
0
1
2
3
Bounding box area (z-scored)
AUC = 0.64
True Positive Rate
1.00
0.75
0.50
0.25
0.00
0.0
0.5
1.0
False Positive Rate

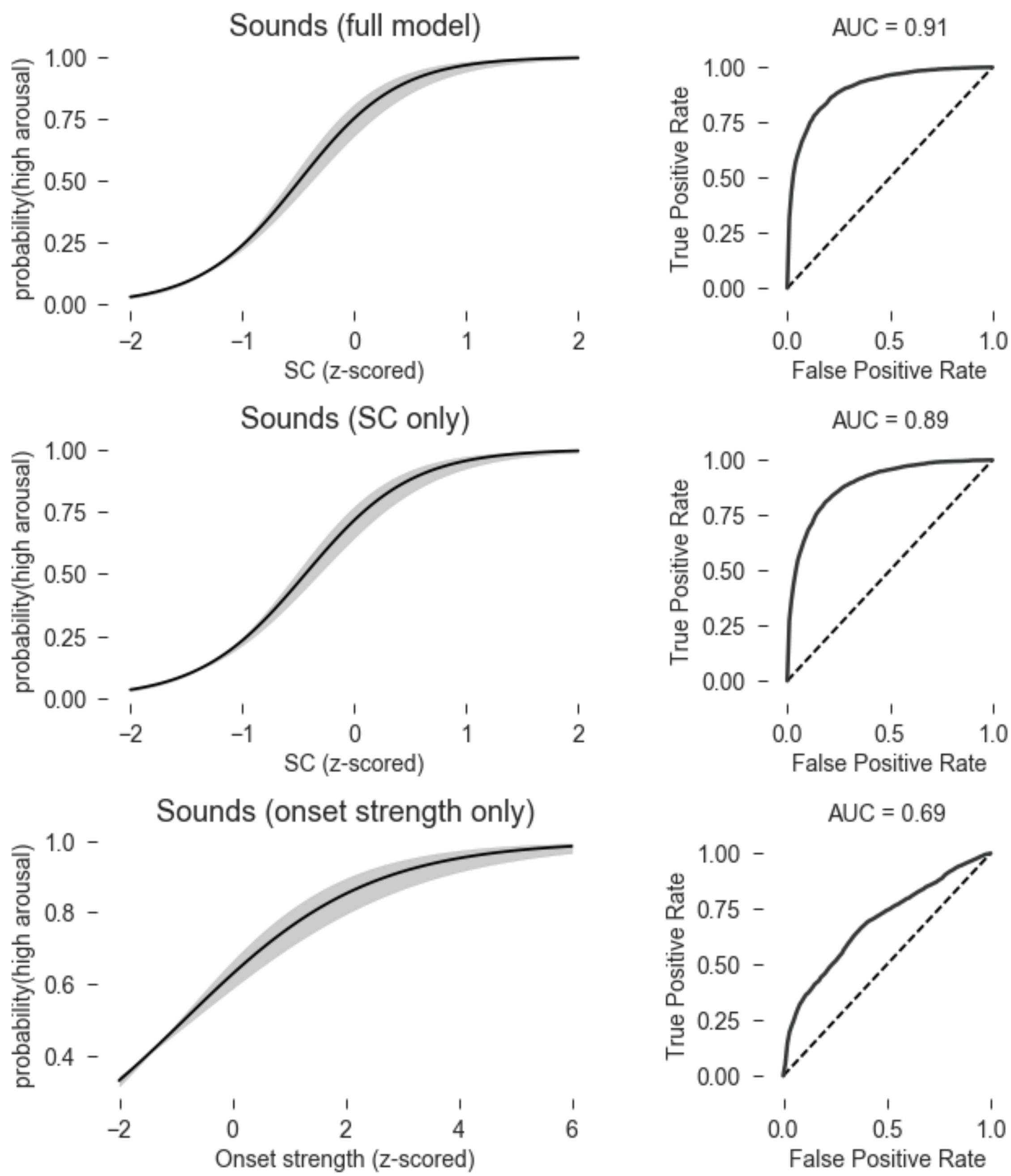

Sounds (full model)
probability(high arousal)
1.00
0.75
0.50
0.25
0.00
−2
−1
0
1
2
SC (z-scored)
AUC = 0.91
True Positive Rate
False Positive Rate
0.0
0.5
1.0
Sounds (SC only)
AUC = 0.89
Sounds (onset strength only)
1.0
0.8
0.6
0.4
4
6
Onset strength (z-scored)
AUC = 0.69

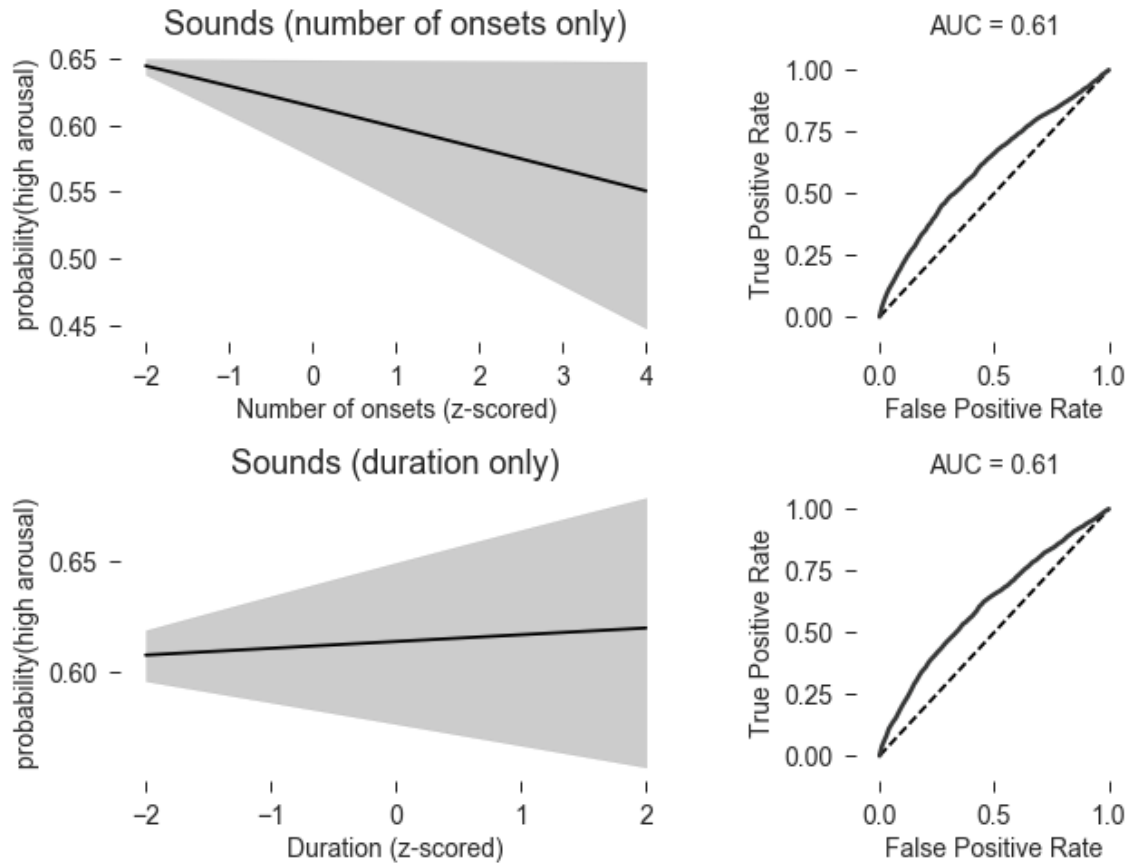

References

Belanger, O. (2016). Pyo, the Python DSP toolbox. *Proceedings of the 2016 ACM on Multimedia Conference*, 1214–1217. https://doi.org/10.1145/2964284.2973804

Carpenter, B., Gelman, A., Hoffman, M., Lee, D., Goodrich, B., Betancourt, M. M. A. B., … Riddell, A. (n.d.). Stan: A probabilistic programming language. *Journal of Statistical Software*.

Davis, R. (1961). The fitness of names to drawings. A cross-cultural study in Tanganyika. *British Journal of Psychology*, *52*(3), 259–268. Retrieved from http://onlinelibrary.wiley.com/doi/10.1111/j.2044-8295.1961.tb00788.x/abstract

Plummer, M. (2003). JAGS: A Program for Analysis of Bayesian Graphical Models Using Gibbs Sampling. *Proceedings of the 3rd International Workshop on Distributed Statistical Computing (DSC 2003). March*, (Dsc), 20–22. https://doi.org/10.1.1.13.3406

R Core Team. (2014). R: A Language and Environment for Statistical Computing. Vienna, Austria. Retrieved from http://www.r-project.org

Rössler, O. E. (1976). An equation for continuous chaos. *Physics Letters A*, *57*(5), 397–398. https://doi.org/10.1016/0375-9601(76)90101-8

Salvatier, J., Wiecki, T., & Fonnesbeck, C. (2016). Probabilistic Programming in Python using PyMC, 1–24. https://doi.org/10.7717/peerj-cs.55

van der Walt, S., Schönberger, J. L., Nunez-Iglesias, J., Boulogne, F., Warner, J. D., Yager, N., … the scikit-image contributors. (2014). scikit-image: image processing in {P}ython. *PeerJ*, *2*, e453. https://doi.org/10.7717/peerj.453

Yarkoni, T., & Westfall, J. (2016). Bambi: A simple interface for fitting Bayesian mixed effects models. https://doi.org/10.17605/OSF.IO/RV7SN

A multi-sensory code for emotional arousal: Study 3 tables

Beau Sievers[a], Caitlyn Lee[b], William Haslett[c] & Thalia Wheatley[b]

[a]Department of Psychology, Harvard University, Cambridge, MA 02138

[b]Department of Psychological and Brain Sciences, Dartmouth College, Hanover, NH 03755

[c]Department of Biomedical Data Science, Geisel School of Medicine at Dartmouth, Hanover, NH 03755

Correspondence to: Thalia Wheatley, 6207 Moore Hall, Dartmouth College, Hanover, NH 03755. thalia.p.wheatley@dartmouth.edu

Description

This document contains summary tables of posterior probabilities for each Bayesian hierarchical logistic regression model in Study 3. For all tables, "bin" refers to the spectral centroid/corner count bin of the stimulus. Boolean categorical factors contain the positive term in their name, e.g., "modalitySound." Terms including "|subID_sd" refer to per-participant random effects. All CIs are 95% credible intervals. The Gelman-Rubin statistic assesses Monte Carlo Markov Chain convergence (Gelman & Rubin, 1992); values close to 1 indicate good convergence.

Bibliography

Gelman, A., and Rubin, D. B. (1992). Inference from Iterative Simulation Using Multiple Sequences. *Statistical Science*, 7, 457–511.

Study 3: The spectral centroid predicts emotional arousal across many shapes and sounds

Multimodal: full model

	M	SD	CI lower	CI upper	Effective N	Gelman-Rubin
1|subID_sd	0.36	0.08	0.22	0.52	1234.4	1
Intercept	0.13	0.09	-0.05	0.31	2090.4	1
bin	1.12	0.1	0.92	1.32	1760	1
bin:modalitySound	0.69	0.15	0.4	1	2337.6	1
bin:modalitySound:positiveValence	0.04	0.28	-0.49	0.6	3094.8	1
bin:modalitySound:positiveValence|subID_sd	0.64	0.3	0.02	1.16	1229.2	1
bin:modalitySound|subID_sd	0.57	0.13	0.34	0.83	1673.6	1
bin:positiveValence	0.72	0.17	0.39	1.04	2265.2	1
bin:positiveValence|subID_sd	0.21	0.15	0	0.48	1345	1
bin|subID_sd	0.42	0.07	0.29	0.56	2335.4	1
modalitySound	0.57	0.22	0.14	0.99	1267.2	1
modalitySound:positiveValence	0.13	0.44	-0.75	0.97	2340.4	1
modalitySound:positiveValence|subID_sd	1.31	0.44	0.36	2.21	1071	1
modalitySound|subID_sd	0.9	0.19	0.58	1.28	878	1
positiveValence	0.38	0.22	-0.05	0.8	2509.4	1
positiveValence|subID_sd	0.75	0.19	0.39	1.15	1793	1

Multimodal: SC

	M	SD	CI lower	CI upper	Effective N	Gelman-Rubin
1|subID_sd	0.45	0.06	0.35	0.57	1348	1
Intercept	0.49	0.08	0.34	0.64	904.6	1
bin	1.61	0.08	1.45	1.77	1160.4	1
bin|subID_sd	0.47	0.06	0.36	0.6	1584	1

Multimodal: modality

	M	SD	CI lower	CI upper	Effective N	Gelman-Rubin
1|subID_sd	0.35	0.05	0.26	0.44	2706	1
Intercept	0.17	0.06	0.05	0.29	4675.4	1
modalitySound	0.3	0.1	0.09	0.49	4083.4	1
modalitySound|subID_sd	0.6	0.08	0.45	0.76	2652.8	1

Multimodal: valence

	M	SD	CI lower	CI upper	Effective N	Gelman-Rubin
1|subID_sd	0.24	0.04	0.16	0.32	1177.6	1
Intercept	0.23	0.06	0.12	0.35	955.2	1
positiveValence	0.14	0.09	-0.04	0.31	1158.4	1
positiveValence|subID_sd	0.13	0.09	0	0.28	476	1

Shapes: full model

	M	SD	CI lower	CI upper	Effective N	Gelman-Rubin
1|subID_sd	0.82	0.11	0.62	1.05	2130.2	1
Intercept	0.51	0.14	0.24	0.78	1434.6	1
areaRatio	-1.23	0.08	-1.39	-1.08	5048.4	1
areaRatio:boundingBoxArea	-0.41	0.06	-0.52	-0.3	6000	1
areaRatio:boundingBoxArea|subID_sd	0.11	0.07	0	0.24	2275.2	1
areaRatio|subID_sd	0.35	0.07	0.22	0.48	2846.6	1
bin	2.16	0.11	1.94	2.38	3239.4	1
bin:areaRatio	-0.05	0.06	-0.17	0.07	6000	1
bin:areaRatio:boundingBoxArea	-0.03	0.06	-0.15	0.08	6000	1
bin:areaRatio:boundingBoxArea|subID_sd	0.09	0.07	0	0.22	2675.4	1
bin:areaRatio|subID_sd	0.17	0.08	0.01	0.31	1546.8	1
bin:boundingBoxArea	-0.61	0.05	-0.7	-0.51	6000	1
bin:boundingBoxArea|subID_sd	0.09	0.06	0	0.2	2359.2	1
bin|subID_sd	0.61	0.09	0.44	0.79	2936.2	1
boundingBoxArea	-0.93	0.1	-1.11	-0.74	2852	1
boundingBoxArea|subID_sd	0.53	0.08	0.38	0.68	2798.6	1

Shapes: SC

	M	SD	CI lower	CI upper	Effective N	Gelman-Rubin
1|subID_sd	0.65	0.09	0.49	0.83	1550.8	1

	M	SD	CI lower	CI upper	Effective N	Gelman-Rubin
Intercept	0.31	0.11	0.1	0.52	816.6	1
bin	1.48	0.1	1.28	1.68	1259.2	1
bin|subID_sd	0.6	0.08	0.45	0.76	1608.2	1

Shapes: convexity

	M	SD	CI lower	CI upper	Effective N	Gelman-Rubin
1|subID_sd	0.46	0.06	0.34	0.58	1924.2	1
Intercept	0.2	0.08	0.05	0.35	2061	1
areaRatio	-0.83	0.05	-0.92	-0.74	4575.4	1
areaRatio|subID_sd	0.22	0.05	0.13	0.31	2295	1

Shapes: bounding box area

	M	SD	CI lower	CI upper	Effective N	Gelman-Rubin
1|subID_sd	0.39	0.05	0.29	0.49	2055	1
Intercept	0.17	0.07	0.04	0.3	2084.4	1
boundingBoxArea	-0.21	0.07	-0.35	-0.07	2117.2	1
boundingBoxArea|subID_sd	0.41	0.06	0.31	0.53	1766.6	1

Sounds: full model

	M	SD	CI lower	CI upper	Effective N	Gelman-Rubin
1|subID_sd	1.01	0.13	0.77	1.28	1422.8	1
Intercept	1.11	0.17	0.77	1.45	708	1
bin	2.26	0.13	2.01	2.52	1836.2	1
bin:duration	-0.33	0.1	-0.51	-0.14	3030	1
bin:duration:numOnsets	-0.07	0.07	-0.2	0.07	4673.8	1
bin:duration:numOnsets:onsetStrength	-0.16	0.08	-0.32	0	4707.6	1
bin:duration:numOnsets:onsetStrength|subID_sd	0.12	0.08	0	0.27	1483.8	1
bin:duration:numOnsets|subID_sd	0.14	0.08	0	0.28	1300.2	1
bin:duration:onsetStrength	-0.37	0.11	-0.59	-0.15	3006.8	1
bin:duration:onsetStrength|subID_sd	0.13	0.08	0	0.28	1580.8	1
bin:duration|subID_sd	0.09	0.06	0	0.2	2047.4	1
bin:numOnsets	0.59	0.12	0.36	0.83	3051.8	1
bin:numOnsets:onsetStrength	0.78	0.14	0.5	1.05	2949.4	1
bin:numOnsets:onsetStrength|subID_sd	0.15	0.09	0	0.31	1613.8	1
bin:numOnsets|subID_sd	0.11	0.07	0	0.24	1728.6	1
bin:onsetStrength	-0.16	0.13	-0.41	0.09	2969.8	1
bin:onsetStrength|subID_sd	0.52	0.1	0.34	0.71	2674.8	1
bin|subID_sd	0.66	0.1	0.47	0.86	2066.8	1
duration	-0.03	0.08	-0.19	0.13	2799.6	1
duration:numOnsets	-0.04	0.05	-0.14	0.06	5919.8	1
duration:numOnsets:onsetStrength	-0.12	0.06	-0.23	-0.01	5723.8	1
duration:numOnsets:onsetStrength|subID_sd	0.08	0.05	0	0.18	1674	1
duration:numOnsets|subID_sd	0.06	0.05	0	0.15	2011.4	1

	M	SD	CI lower	CI upper	Effective N	Gelman-Rubin
duration:onsetStrength	-0.18	0.1	-0.37	0.01	2730.6	1
duration:onsetStrength|subID_sd	0.21	0.07	0.07	0.35	1436.4	1
duration|subID_sd	0.09	0.06	0	0.19	1766.4	1
numOnsets	0.14	0.1	-0.05	0.34	2875.2	1
numOnsets:onsetStrength	0.48	0.11	0.27	0.7	2807.4	1
numOnsets:onsetStrength|subID_sd	0.18	0.08	0.02	0.33	1088.8	1
numOnsets|subID_sd	0.11	0.06	0	0.22	1499.8	1
onsetStrength	0.69	0.12	0.46	0.92	1716.6	1
onsetStrength|subID_sd	0.58	0.09	0.42	0.76	2066.6	1

Sounds: SC

	M	SD	CI lower	CI upper	Effective N	Gelman-Rubin
1|subID_sd	0.95	0.12	0.72	1.19	997.2	1
Intercept	0.92	0.16	0.6	1.22	574.8	1
bin	2.11	0.11	1.9	2.34	1237.4	1
bin|subID_sd	0.63	0.09	0.46	0.81	1536	1

Sounds: mean onset strength

	M	SD	CI lower	CI upper	Effective N	Gelman-Rubin
1|subID_sd	0.49	0.07	0.37	0.63	1818.2	1
Intercept	0.52	0.08	0.36	0.68	1582.2	1
onsetStrength	0.61	0.06	0.5	0.73	3301	1
onsetStrength|subID_sd	0.31	0.05	0.22	0.41	2463	1

Sounds: number of onsets

	M	SD	CI lower	CI upper	Effective N	Gelman-Rubin
1|subID_sd	0.46	0.06	0.35	0.59	1631.8	1
Intercept	0.47	0.08	0.31	0.62	1364.2	1
numOnsets	-0.07	0.03	-0.13	-0	5580.8	1
numOnsets|subID_sd	0.13	0.04	0.05	0.21	1792.6	1

Sounds: duration

	M	SD	CI lower	CI upper	Effective N	Gelman-Rubin
1|subID_sd	0.46	0.06	0.35	0.58	1477.4	1
Intercept	0.46	0.08	0.31	0.62	1129.6	1
duration	0.01	0.03	-0.04	0.07	5979.2	1
duration|subID_sd	0.07	0.04	0	0.14	1512.4	1

Study 5: Continuous arousal across emotions

	M	SD	CI lower	CI upper	Effective N	Gelman-Rubin
1|subID_sd	0.06	0.01	0.03	0.09	2158.8	1
Intercept	0.15	0.02	0.11	0.19	4727.4	1
arousalRating	0.76	0.03	0.71	0.81	2467.4	1
arousalRating:modalitySound[T.1]	-0.22	0.02	-0.27	-0.18	5628.6	1
arousalRating|subID_sd	0.12	0.02	0.09	0.16	2062.2	1
modalitySound[T.1]	-0.27	0.02	-0.3	-0.23	5993.2	1
sc_sd	0.83	0.01	0.82	0.85	6000	1
valenceRating	-0.09	0.02	-0.13	-0.05	4585.4	1
valenceRating:arousalRating	-0.1	0.01	-0.13	-0.07	5340.8	1
valenceRating:arousalRating:modalitySound[T.1]	0.15	0.02	0.11	0.18	5204.2	1
valenceRating:modalitySound[T.1]	-0.06	0.02	-0.11	-0.02	5001.6	1
valenceRating|subID_sd	0.05	0.02	0.02	0.08	1722.8	1